Effect of Neutrophil Adhesion on the Mechanical Properties of Lung Microvascular Endothelial Cells

Inkyung Kang[1]*, Qin Wang[1]†, Steven J. Eppell[1], Roger E. Marchant[1], and Claire M. Doerschuk[1,2]

[1]Department of Biomedical Engineering, and Division of Integrative Biology, Department of Pediatrics, Case Western Reserve University, Cleveland, Ohio; and [2]the Center for Airways Disease and Department of Medicine, University of North Carolina Chapel Hill, Chapel Hill, North Carolina

Neutrophil adhesion to pulmonary microvascular endothelial cells (ECs) initiates intracellular signaling, resulting in remodeling of F-actin cytoskeletal structure of ECs. The present study determined the mechanical properties of ECs and the changes induced by neutrophil adhesion by atomic force microscopy. The elastic moduli of ECs were compared before neutrophils were present, as soon as neutrophil adhesion was detected, and 1 minute later. ECs that were adjacent to those with adherent neutrophils were also evaluated. Neutrophil adhesion induced a decrease in the elastic moduli in the 6.25-μm rim of ECs surrounding adherent neutrophils as soon as firmly adherent neutrophils were detected, which was transient and lasted less than 1 minute. Adjacent ECs developed an increase in stiffness that was significant in the central regions of these cells. Intercellular adhesion molecule–1 crosslinking did not induce significant changes in the elastic modulus of ECs in either region, suggesting that crosslinking intercellular adhesion molecule–1 is not sufficient to induce the observed changes. Our results demonstrate that neutrophil adhesion induces regional changes in the stiffness of ECs.

Keywords: neutrophils; pulmonary microvascular endothelial cells; mechanical properties; intercellular adhesion molecule–1

Interactions between neutrophils and pulmonary microvascular endothelial cells (ECs) are one of the first events during host defense. This interaction is often mediated through binding of CD11a/CD18 and CD11b/CD18 (integrin-$\alpha_L\beta_2$ and -$\alpha_M\beta_2$) on neutrophils to intercellular adhesion molecule (ICAM)–1 on ECs. Intracellular signaling cascades initiated by neutrophil adhesion are mediated by p38 mitogen-activated protein kinase, and result in increased F-actin levels in ECs (1–3). This signaling results in stiffening of ECs within 2 minutes, as measured by magnetic bead twisting cytometry. Inhibition of p38 activity attenuates neutrophil migration along ECs to their borders. The intracellular signaling events initiated by neutrophil adhesion to pulmonary microvascular ECs are closely mimicked by crosslinking ICAM-1 using anti–ICAM-1 antibodies and a secondary anti-Fc antibody (2).

Atomic force microscopy (AFM) measures the displacement of a sample that results from the force applied by the AFM probe. Mechanical properties of living cells are determined by analyzing the relationship between the loading force and the displacement of the cell (4, 5). Force-indentation curves obtained at each x, y position of the entire surface of the cell are assembled into a map of elastic moduli, which is then correlated with the topography of the cell. AFM studies have measured the mechanical properties of living cells in the time course of biological processes (e.g., the real-time changes in micromechanical properties of human umbilical vein ECs during monocyte adhesion [6], the elastic moduli of human embryonic kidney cells during stimulation with angiotensin II [7], the elastic moduli of human mesenchymal stem cells during osteogenic differentiation [8], and the apparent elastic modulus of skeletal muscle cells throughout differentiation [9]). The observations that intracellular signaling in ECs initiated by neutrophil adhesion results in local alteration in the F-actin cytoskeleton, and is critical for neutrophil migration to EC borders, led to the hypothesis that neutrophil adhesion leads to regional changes in the mechanical properties of ECs.

The present study determined the mechanical properties of cultured pulmonary microvascular ECs and the global and regional changes induced by neutrophil adhesion and by ICAM-1 crosslinking by AFM. The mechanical properties were quantified by calculating the elastic modulus for each force-displacement curve. Our data demonstrate that, soon after neutrophil adhesion, the stiffness of ECs decreased in the EC rim surrounding the adherent neutrophils. This decreased stiffness lasts less than 1 minute. The adjacent ECs show no significant change soon after neutrophil adhesion to their neighbor, but 1 minute later, their stiffness is increased, particularly in the central regions. ICAM-1 crosslinking over the entire EC surface did not induce a significant change in the apparent stiffness of ECs. Our findings demonstrate that neutrophil adhesion induces regional changes in the stiffness of ECs.

CLINICAL RELEVANCE

Neutrophil adhesion and migration along endothelial cells (ECs) and into the lung tissue occur in all pulmonary diseases in which the acute inflammatory response contributes. These studies demonstrate that neutrophil adhesion induces signaling processes that modulate EC mechanics.

MATERIALS AND METHODS

Cell Culture

Human pulmonary microvascular ECs were purchased from Cambrex (Walkersville, MD), and plated on fibronectin-coated 35-mm cell culture polystyrene dishes, according to the manufacturer's protocols. Confluent ECs between passages 7 and 15 were studied. ECs were exposed to TNF-α (20 ng/ml) overnight before experiments to increase neutrophil adhesion and to mimic the inflammatory process.

Neutrophil Isolation

Blood was collected by venipuncture from healthy donors after informed consent was obtained. Human neutrophils were isolated from blood with histopaque density gradients (Sigma, St. Louis, MO), according to the manufacturer's protocol.

(*Received in original form October 10, 2006 and in final form October 19, 2009*)

This work was supported by National Heart, Lung, and Blood Institute grants HL070009 (Q.W.), and HL048160 and HL077370 (C.M.D.).

* Current address for I.K.: Benaroya Research Institute at Virginia Mason, 1201 9th Ave., Seattle WA 98101

† Current address for Q.W.: Department of Surgery, Mount Sinai Medical Center, One Gustave L. Levy Place, New York, NY 10029

Correspondence and requests for reprints should be addressed to Claire M. Doerschuk, M.D., 7011 Thurston Bowles, CB #7248, University of North Carolina Chapel Hill, Chapel Hill, NC 27599-7248. E-mail: cmd@med.unc.edu

Am J Respir Cell Mol Biol Vol 42. pp 591–598, 2010
Originally Published in Press as DOI: 10.1165/rcmb.2006-0381OC on December 18, 2009
Internet address: www.atsjournals.org

AFM

AFM force maps of ECs were obtained with a Nanoscope IV Bioscope AFM (Digital Instruments, Santa Barbara, CA) equipped with a G-type scanner. AFM images and force maps were obtained with silicon nitride probes of 0.06 N/m (Digital Instruments) while the cells were covered with culture medium. Briefly, AFM force–displacement curves were measured at every pixel on a topographic image of the cells. Mechanical properties were calculated as the elastic modulus from each force–displacement curve (*see below*), and the elastic moduli were arranged into maps corresponding to the spatial position of each x, y pixel in the image.

Analysis of Cell Thickness from AFM Force-Displacement Data

Force-displacement data were obtained from the AFM force–displacement curves, which record the AFM cantilever deflection against the displacement of the Z-piezo, as previously discussed (5). Briefly, the force was calculated as the cantilever deflection multiplied by the spring constant of the cantilever (nominal value of 0.06 N/m), and the displacement of the cell was calculated as the Z-piezo displacement minus the deflection of the cantilever.

The thickness of ECs was determined from the topography, and indentation depth from the force-displacement curve of each pixel. The thickness was calculated as (10):

$$\text{thickness}_{\text{pixel}} = \text{z-height}_{\text{pixel}} - \text{z-height}_0 + \max(\text{indentation depth})_{\text{pixel}},$$

where $\text{z-height}_{\text{pixel}}$ is the piezo z-height of each pixel from the AFM topographic image; z-height_0 is the smallest piezo z-height among all the pixels in the AFM topographic image; $\max(\text{indentation depth})_{\text{pixel}}$ is the maximum indentation depth determined for each pixel from the force-displacement data.

The maximum indentation depth is calculated for each force-displacement curve as:

$$\max(\text{indentation depth}) = \text{z-height}_{\text{contact}} - \text{z-height}_{\text{max displacement}} - \max(\text{cantilever deflection}),$$

where $\text{z-height}_{\text{contact}}$ is the z-height of piezo at the point of contact; $\text{z-height}_{\text{max displacement}}$ is the z-height of piezo at which the displacement of the cell underneath the AFM probe reaches its maximum; max(cantilever deflection) is the maximum deflection of cantilever.

Analysis of Elastic Moduli from AFM Force-Displacement Data

Apparent elastic moduli were determined by optimizing the elastic moduli parameter, E, in the following equations based on Hertz's contact theory to minimize the difference between the theoretical force–displacement equations and the experimental AFM data (Figure 1). The contact between the AFM probe and the EC monolayer was modeled as a conical indenter with a spherical tip in contact with an elastic half space. The force–displacement relationships during the contact of rigid blunt-conical indenter and an elastic half space can be expressed as previously described (11):

$$\text{When } w_0 \leq \frac{b^2}{R},$$
$$F = \frac{4E}{3(1-\nu^2)} R^{1/2} w_0^{3/2};$$
$$\text{when } w_0 \geq \frac{b^2}{R},$$
$$F = \frac{2E}{(1-\nu^2)}\left\{ a w_0 - \frac{a^2}{2\tan\theta}\left[\frac{\pi}{2} - \arcsin\left(\frac{b}{a}\right)\right] - \frac{a^3}{3R} + (a^2-b^2)^{1/2}\left(\frac{b}{2\tan\theta} + \frac{a^2-b^2}{3R}\right)\right\}$$

with the contact radius, a, calculated from the following equation:

$$w_0 + \frac{a}{R}\left((a^2-b^2)^{1/2} - a\right) - \frac{a}{\tan\theta}\left[\frac{\pi}{2} - \arcsin\left(\frac{b}{a}\right)\right] = 0,$$

where F is applied force, E is apparent elastic modulus of the elastic half-space, ν is Poisson's ratio, a is contact radius, b is the point along the axis perpendicular to the tip's axis of symmetry where the transition between cone and sphere occurs ($R\cos\theta$), R is the radius of a sphere (100 nm), w_0 is indentation depth, and θ is the half-open angle of a cone (nominal value of 37.5° for the standard silicon nitride cantilever).

Curve fitting was performed in Matlab 7.0 (The MathWorks, Natick, MA) with the Nelder-Mead simplex algorithm (12). Values of E with zero or negative coefficient of correlation ($R^2 \leq 0$) between the data and the theoretical model were excluded.

To compare the mechanical response of the ECs by using different indentation depths, the apparent elastic moduli were categorized according to the depth of indentation used in the optimization: $E_{0\text{–}100\ \text{nm}}$ for indentation depths 0–100 nm; $E_{>100\ \text{nm}}$ for indentation depths greater than 100 nm; and E_{total} for the total indentation depths.

Effects of Neutrophil Adhesion and Migration on the Mechanical Properties of ECs

To determine the effect of neutrophil adherence to ECs, changes in the elastic moduli of ECs and neutrophils were determined before and during neutrophil adhesion and migration in time-series maps of elastic moduli obtained every minute from 2 to 6 minutes after neutrophil adhesion (1×10^6 per 35-mm culture dish; >95% purity). All AFM images were taken at 37°C. AFM force maps were obtained in a square area of 100 μm^2 containing 16×16 pixels (6.25×6.25 μm per pixel). Each curve was collected with a stroke of 1 μm and a cycling time of

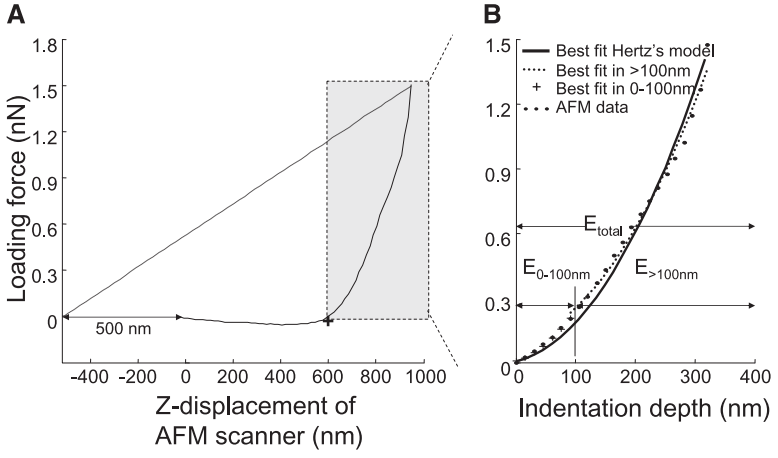

Figure 1. Force-displacement curves obtained during a single indentation with atomic force microscopy (AFM). (*A*) The contact point (+) between the AFM probe and the endothelial cell (EC) was identified in the force-displacement curve as the point where the difference between the force-displacement curve and a straight line drawn from a point offset from the starting point by 500 nm on the x-axis (x_{0-500}, y_0) and the last point of the curve is maximal. The *shaded rectangle* denotes the in-contact region where the AFM probe was applying force to the cells. (*B*) Apparent elastic moduli were determined by optimization of the elastic modulus parameter in the force-displacement equation given by Hertz's and Sneddon's infinitesimal strain theory. The value of E that provided a positive correlation ($R^2 > 0$) between the data and the theoretical model was considered the elastic modulus for that pixel. The elastic moduli were determined in different ranges of indentation depths: $E_{0\text{–}100\ \text{nm}}$ for the indentation depth 0–100 nm; $E_{>100\ \text{nm}}$ for the indentation depth greater than 100 nm; and E_{total} for the entire indentation depth.

0.125 second. A topographic map was simultaneously generated with the cantilever deflection signal at maximum stroke over each pixel. The presence of adherent neutrophils and their migrating directions were detected from the thickness maps reconstructed from the topographic information, and the force-displacement curve from each pixel, as described previously here.

An adherent neutrophil was identified when two criteria were met: (*1*) more than three neighboring pixels increased in height by at least 1 μm compared with their height before neutrophil adhesion; and (*2*) this increase in thickness remained within 0–10 μm for at least two images (1 min apart). An increase in thickness of more than 1 μm was chosen to represent a neutrophil following comparisons of two topographic maps obtained from AFM measurements performed 1 minute apart with the same ECs, but without addition of neutrophils. The Gaussian distribution of the differences between these two sequential measurements of height for each pixel had an average of −0.13 (±0.10) μm and the SD of 0.45 (±0.04) μm (n = 5). Thus, an increase in height greater than twice this SD value in three neighboring pixels was considered to be due to an adherent neutrophil. This approach may result in missing adherent neutrophils (false negatives), but false positives that result in identifying a neutrophil when none is present are very unlikely.

ECs were considered to be adjacent to ECs with adherent neutrophils when: (*1*) more than 25 μm of their border was in contact with an EC to which a neutrophil had adhered; and (*2*) all or a large portion of the EC that included the central and peripheral regions was within the AFM field.

The topographic map was used to divide each EC into peripheral (within 10 μm from the intercellular junctions between neighboring ECs) and central regions with ImageJ (National Institutes of Health, Bethesda, MD) to determine the properties of these subcellular regions. The pixels (6.25-μm square) immediately surrounding the adherent neutrophils were categorized as rim 1 and rim 2 (Figure 2). These rims were further divided into four subregions according to the direction of neutrophil migration: the migrating direction, the opposite direction, and the directions perpendicular to the axis of migration (Figure 2). Apparent elastic moduli of these regions (central, peripheral, rim 1, and rim 2) were determined at three time points: (*1*) before adding neutrophils (baseline); (*2*) after neutrophils were allowed to adhere for 2 minutes and as soon as neutrophil adhesion was detected from the thickness images (at firm adhesion); and (*3*) in the consecutive image (1 min later). Apparent elastic moduli of the four subregions were determined at two time points: (*1*) before adding neutrophils (baseline); and (*2*) after neutrophils adhered for 1 minute and before their migration was detected from the AFM topography images (onset of migration). To determine the changes in the elastic moduli after neutrophil adhesion compared with the baseline values, the same pixels before and after adding neutrophils were compared for each region and each time point, and the areas occupied by adherent neutrophils were excluded from both the baseline maps and the maps after neutrophil adhesion. Median and interquartile range of elastic moduli were calculated from the elastic moduli map of each region using a custom-written code in Matlab 7.0.

Changes in the Mechanical Properties of ECs Induced by ICAM-1 Crosslinking

To determine the effect of ICAM-1 crosslinking on the changes in mechanical properties of ECs, the following experiments were performed.

ECs were incubated with murine monoclonal anti–human ICAM-1 antibodies (6.65 μg/ml; Dako, Carpinteria, CA) or 0.1% BSA in PBS for 0.5 hour, followed by washing with culture medium. Immediately before AFM imaging, secondary antibody (goat F(ab′)2 anti-mouse IgG F(C), 50 μg/ml; ICN/Cappel, Irvine, CA) or 0.1% BSA in PBS was added. To determine the effect of ICAM-1 crosslinking, four groups were compared: (*1*) buffer control group treated with 0.1% BSA in PBS instead of antibodies; (*2*) secondary control group treated with 0.1% BSA in PBS, followed by secondary antibody; (*3*) primary control group treated with anti–ICAM-1 antibody, followed by 0.1% BSA in PBS; and (*4*) ICAM-1 crosslinked group treated with anti–ICAM-1 antibody, followed by secondary crosslinking antibody.

All ICAM-1 crosslinking experiments were performed at room temperature (25°C). The AFM force map was obtained in a square area of 100 μm^2 immediately after the crosslinking antibody was added or control treatments were finished. Each data set consisted of a 64 × 64 array of force-indentation curves (1.56 × 1.56 μm per data point). Each curve was collected using a stroke of 1 μm and a cycling time of 0.125 second. Collection of the entire array took 20 minutes from start to finish. The entire EC or the peripheral (within 10 μm from the border) and central (excluding the regions over the nucleus) regions of each EC were outlined from the topographic AFM images with ImageJ. Regions near the nucleus were excluded in the analysis, as the height of the region often exceeded the vertical scanning range of AFM (6 μm). An elastic moduli map was derived from each region with a custom-made program in Matlab 7.0. Median, interquartile range, and skewness of elastic moduli were calculated from the elastic moduli map derived from each region, also employing a custom-made program in Matlab 7.0.

Summary of Analysis of Elastic Moduli

For studies determining the effect of neutrophil adhesion and migration on ECs, the median E_{total} values were calculated for the entire surface and for the peripheral and central regions, as well as for the regions around neutrophils (rim 1 and rim 2). Moreover, the average E_{total} values were calculated in the four subregions of rim 1 and rim 2 determined by the direction of neutrophil migration, E_{mig}, E_{opp}, E_{90}, and E_{270}. For studies of ICAM-1 crosslinking in ECs, the elastic moduli were determined with different indentation depths: $E_{0–100\ nm}$ for indentation depths 0–100 nm; $E_{>100\ nm}$ for indentation depths greater than 100 nm; and E_{total} for the total indentation depths. The median $E_{0–100\ nm}$, $E_{>100\ nm}$, and E_{total} values were calculated for the entire surface and for the peripheral and central regions.

Statistical Analysis

All data are expressed as medians (± interquartile range) unless otherwise specified. Interquartile range is defined as the value of the third

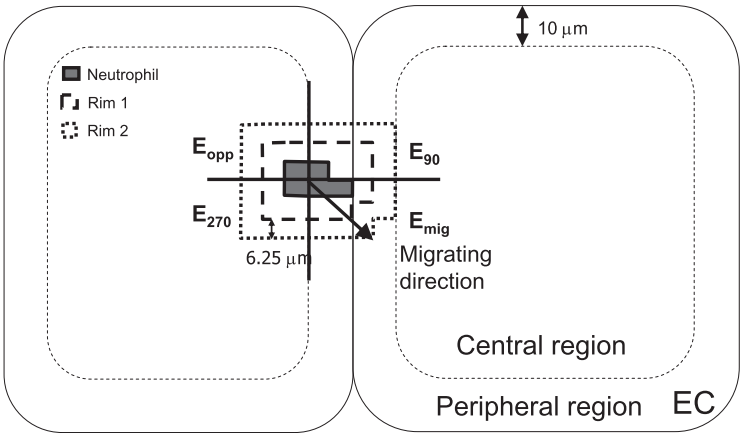

Figure 2. Apparent elastic moduli of ECs during neutrophil adhesion and migration were determined in central and peripheral regions of ECs, as well as in quadrants around adherent neutrophils. The elastic moduli were determined in the peripheral regions within 10 μm of EC borders and in the central regions excluding the area near the nucleus. The elastic moduli were also determined in the EC regions immediately surrounding the adherent neutrophils. Rim 1 consisted of the first pixels around neutrophils (within 0–6.25 μm from the adherent neutrophils). Rim 2 consisted of the second pixels around neutrophils (from 6.25 to 12.50 μm). The rims around neutrophils were divided into four subregions according to the direction of neutrophil migration, and the elastic moduli of each subregion were determined in the migrating direction (E_{mig}), in the opposite direction (E_{opp}), and perpendicular to the axis of migrating direction (E_{90}, E_{270}).

quartile minus the value of the first quartile. The skewness of elastic moduli was calculated to determine the distribution: normally distributed values have the skewness of 0, and a positive skewness value indicates that the values are skewed right, which means that the right tail is longer than the left tail. Because the mechanical properties over the surface of ECs were found to be right skewed, nonparametric statistics were used to analyze elastic moduli, except for the four quadrants of regions around adherent neutrophils, where the number of samples was small. The Sign test and Wilcoxon's matched-pair test were used to compare two dependent measures; for example, comparison of the elastic moduli before and after adding neutrophils, and two different regions of the same cell. The Mann-Whitney U test and Kolmogorov-Smirnov test were used to compare two independent measures. The Kruskal-Wallis ANOVA was used for comparison of more than two independent measures. Changes were regarded as significant if the *P* value was less than 0.05.

RESULTS

Changes in the Mechanical Properties of ECs during Neutrophil Adhesion and Migration

To determine the effects of neutrophil adhesion and migration on the mechanical properties of ECs, these properties were determined before and during neutrophil adhesion and migration. The mechanical properties were measured over the entire EC surface, and were analyzed in the central and peripheral regions, as well as in the regions around adherent neutrophils. The mechanical properties of ECs were determined as the apparent elastic moduli calculated from the force-displacement curves obtained in each cell before and 2 to 6 minutes after neutrophils were added to the EC media. Changes were identified by comparing the elastic moduli of EC regions soon after neutrophil adhesion and 1 minute later to the baseline values measured in the same regions before adding neutrophils. $E_{0–100\ nm}$ of ECs in regions around adherent neutrophils were not available, due to increased noise and decreased resolution of the force-displacement data obtained in the presence of neutrophils. Thus, only E_{total} was used in the analysis of EC response during neutrophil adhesion and migration.

The effect of neutrophil adhesion on the E_{total} of ECs was determined in the regions surrounding the adherent neutrophils, designated rim 1 and 2 (Figure 2). Neutrophil adhesion induced a significant decrease in rim 1 as soon as firm adhesion of neutrophils was detected (Figure 3A), but not in rim 2 (Figure 3B). This change was transient, and was not present 1 minute later. The thickness in rim 1 and rim 2 did not exhibit significant changes at neutrophil adhesion or afterwards (data not shown).

The mechanical properties of the entire EC and the peripheral and central regions were examined, and the effects of neutrophil adhesion were determined. Figure 4 shows the data from these studies normalized to baseline values before neutrophil adhesion. All neutrophils were adherent to the peripheral region at the time of firm adhesion. Neutrophil adhesion induced no significant change in E_{total} in either the peripheral or the central regions upon firm adhesion or by 1 minute later (Figures 4A and 4B). In contrast, ECs adjacent to the ECs displaying adherent neutrophils showed an increase in E_{total} at 1 minute after firm adhesion, which was not yet apparent upon firm adhesion (Figures 4C and 4D). This increase was significant in the central regions of these ECs. These data suggest that neutrophil adhesion induced rapid local changes in the mechanical properties of ECs to which they were bound, and also impacted more diffusively on the mechanical properties of adjacent ECs.

The thickness of ECs to which neutrophils were adherent did not change in any region at the time of firm adhesion or 1 minute later, compared with their thickness before neutrophil adhesion (Figures 5A and 5B) In contrast, the adjacent ECs demonstrated first a decrease in thickness of 11% upon firm adhesion of neutrophils to their neighbor, and then an increase to 8 to 30% of their baseline value after 1 minute (Figures 5C and 5D).

To determine the regional changes in the mechanical properties of ECs upon neutrophil migration, images were selected of time points at the onset of migration, when the neutrophils had adhered for 2 minutes, but before their migration was detectable. The elastic moduli were compared in the migrating direction (E_{mig}), the opposite direction (E_{opp}), or the perpendicular directions (E_{90}, E_{270}) of rim 1 with the elastic moduli of these same regions before adhesion of neutrophils (Figure 2). Adhesion of neutrophils did not change the average elastic moduli of any of the four subregions (data not shown). The average elastic moduli in the quadrants were not significantly different from each other at baseline, or at the onset of neutrophil migration. No significant changes in elastic moduli were observed in rim 2 (data not shown).

ICAM-1 Crosslinking Did Not Induce Significant Changes in the Elastic Moduli of ECs

To determine the effects of ICAM-1 crosslinking on elastic moduli of ECs, the elastic moduli from the three control groups (buffer, secondary antibody alone, and primary antibody alone) and the ICAM-1 crosslinked ECs were compared. Figures 6A and 6B show a representative topographic image and map of elastic moduli of TNF-α–treated ECs. Brighter regions in the images represent the areas that are taller in the topographic images or stiffer in the maps of elastic moduli, as indicated in the scale bar on the right. Topographic images demonstrated that the EC monolayers were confluent, with occasional small gaps exposed between the neighboring ECs due to the effects of TNF-α (13). Elastic moduli could not be determined in some

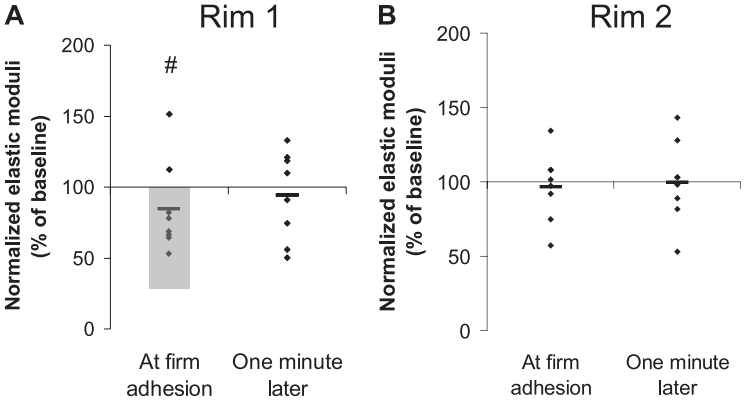

Figure 3. Changes in the E_{total} of the EC regions surrounding adherent neutrophils. The changes were determined by comparing the elastic moduli of rim 1 and rim 2 around adherent neutrophils compared with the baseline values (*please see* Figure 2 for definition of these regions). (*A*) The stiffness in rim 1 significantly decreased at firm adhesion (*shaded area* in *A*; $^{\#}P < 0.05$ in Wilcoxon's matched-pair test). This change was transient, and was not observed 1 minute later. (*B*) No change was observed in rim 2.

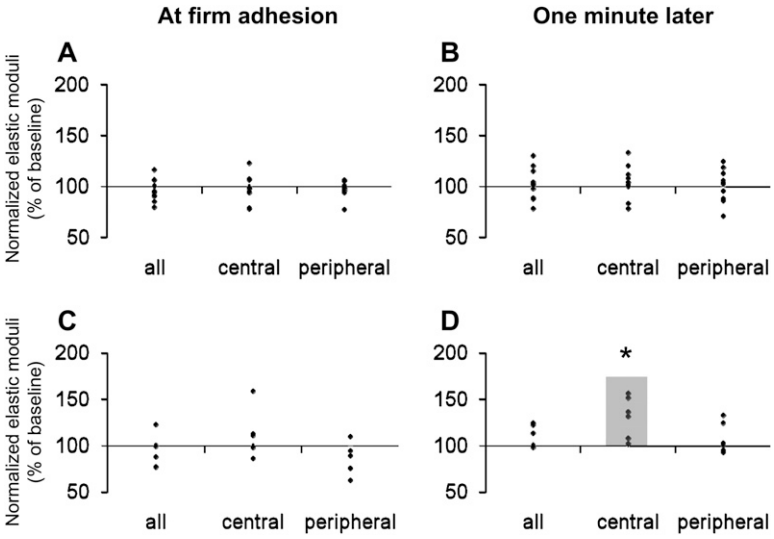

Figure 4. Changes in the E_{total} of EC regions soon after neutrophil adhesion and 1 minute later. The changes were assessed by comparing the values of elastic moduli and the thickness after neutrophil adhesion compared with the baseline values before adding neutrophils; the difference was regarded as significant if *P* was less than 0.05 in Wilcoxon's matched-pair test or in sign test. The elastic moduli after neutrophil adhesion were normalized as a percentage of the baseline values in the same region before adding neutrophils. (*A* and *B*) ECs to which neutrophils were adherent. Neutrophil adhesion induced no significant changes in the E_{total} in either the central or the peripheral regions of the ECs at the time that firm adhesion was first detected (*A*) or 1 minute later (*B*). All neutrophils ($n = 8$) were located at the peripheral regions of ECs at firm adhesion ($n = 10$ ECs from 7 monolayers). (*C* and *D*) ECs adjacent to the ECs on which neutrophils were adherent. Adjacent ECs showed no change in E_{total} at the time when firm adhesion was identified (*C*). However, within 1 minute, neutrophil adhesion induced an increase in stiffness that was significant in the central regions of the adjacent ECs (*D*) ($n = 6$ ECs). *$P < 0.05$ by the sign test and Wilcoxon's matched-pair test when the raw values were compared.

regions near the nuclei, due to the limited scanning range of AFM in the vertical direction (6 μm). The regions above the nuclei (tallest area of each cell in topography) were not included in calculating the average elastic moduli.

The distribution of the apparent elastic moduli was determined for all data points in the entire surface of each TNF-α–treated EC. A representative dot plot of the apparent elastic moduli of the entire surface of an EC indicates that the apparent elastic moduli were not normally distributed (Figure 6C). The median skewness for E_{total}, $E_{0–100\ nm,}$ and $E_{>100\ nm}$ were 0.81 (±0.14), 1.47 (±0.38), and 0.91 (±0.18), respectively, indicating that the distribution of all three elastic moduli was skewed to the right.

To determine the subcellular properties of the ECs, each EC was divided into peripheral (within ~10 μm from cell borders) and central regions. The median value of the apparent elastic moduli was determined for the entire surface and for the central and peripheral regions (Figure 6D). The median $E_{0–100\ nm}$ (but not $E_{>100\ nm}$) values of peripheral regions were significantly greater than those of central regions. $E_{>100\ nm}$ was significantly greater than $E_{0–100\ nm}$ over the entire surface and in the central and peripheral regions.

The effects of ICAM-1 crosslinking on elastic moduli of ECs were determined by comparing the elastic moduli maps from the three control groups (buffer, secondary antibody alone, and primary antibody alone) and the ICAM-1 crosslinked ECs. The median E_{total}, $E_{0–100\ nm}$, and $E_{>100\ nm}$ of ECs after ICAM-1 crosslinking or control treatments were determined for the entire surface of the ECs or for the peripheral and central regions (Figures 7A–7I). No significant differences were found between ICAM-1 crosslinked ECs and the three controls for E_{total}, $E_{0–100\ nm}$, or $E_{>100\ nm}$ for the entire surface or for the central or peripheral regions when tested with Kruskal-Wallis ANOVA. The skewness of E_{total}, $E_{0–100\ nm}$, and $E_{>100\ nm}$ of ICAM-1 crosslinked ECs was not significantly different from that of controls. These findings indicate that ICAM-1 crosslinking did not induce significant changes in the elastic moduli of ECs.

DISCUSSION

The present study tested the hypothesis that neutrophil adhesion alters the mechanical properties of pulmonary microvascular ECs. The mechanical properties were measured by calculating the apparent elastic moduli with force-displacement curves obtained by AFM. Our results demonstrate that neutrophil

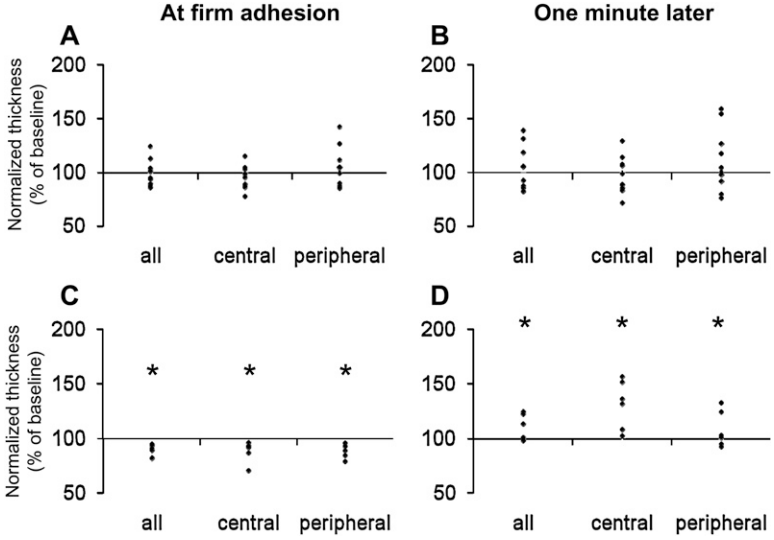

Figure 5. Changes in the thickness of EC regions soon after neutrophil adhesion and 1 minute later compared with their thickness before neutrophil adhesion. (*A* and *B*) ECs to which neutrophils were adherent. Neutrophil adhesion induced no significant changes in the thickness of any EC region at the time when firm adhesion was first detected (*A*) or 1 minute later (*B*) ($n = 10$ ECs from 7 monolayers). (*C* and *D*) ECs adjacent to the ECs on which neutrophils were adherent. Adjacent ECs showed a significant decrease in thickness at the time when firm adhesion was identified (*C*). Within 1 minute, the thickness of these adjacent ECs had increased to values above the baseline value before neutrophil adhesion (*D*) ($n = 6$ ECs). *$P < 0.05$ by the sign test and Wilcoxon matched-pair test.

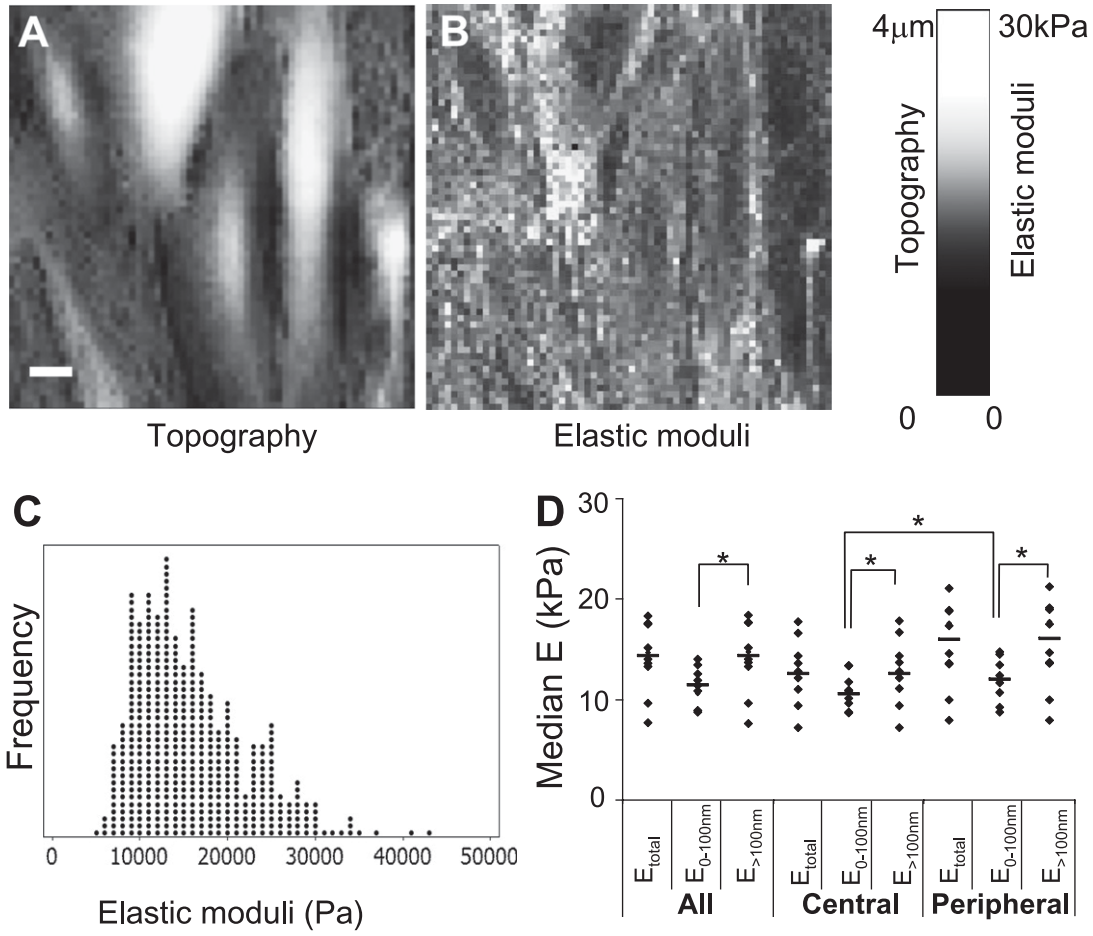

Figure 6. Representative *topographic image* (*A*), *map* of elastic moduli (*B*), *dot plot* of elastic properties over the entire surface of a TNF-α–treated EC (*C*), and median E_{total}, $E_{0–100\ nm}$, and $E_{>100\ nm}$ of TNF-α–treated ECs (*D*). (*A* and *B*) In the *topographic image* and *map* of elastic moduli, the Z height and elastic modulus of each pixel is represented as the brightness of that pixel in respective images, as shown in the *scale bar* on the *right*. The *scale bar* in the topographic image represents 10 μm. (*C*) The *dot plot* of all elastic moduli values of a single TNF-α–treated EC shows that these moduli are not normally distributed, but are right-skewed. (*D*) The median E_{total}, $E_{0–100\ nm}$, and $E_{>100\ nm}$ of the entire surface and of the central and peripheral regions of TNF-α–treated ECs were compared. $E_{>100\ nm}$ was significantly greater than $E_{0–100\ nm}$ in both the central and the peripheral regions (*$P < 0.05$ in sign test and Wilcoxon's matched-pair test). $E_{0–100\ nm}$ of the peripheral regions were significantly greater than those of the central regions (*$P < 0.05$ in sign test and Wilcoxon's matched-pair test).

adhesion initially decreases the stiffness transiently in ECs immediately surrounding adherent neutrophils (EC rim 1). This change was statistically significant when the raw elastic moduli were compared with the baseline values. The decreases in the mechanical properties were transient, and were over by 1 minute after firm adhesion. Adherent neutrophils also altered adjacent ECs, resulting in an increased stiffness that was significant in the central regions. Mimicking neutrophil adhesion

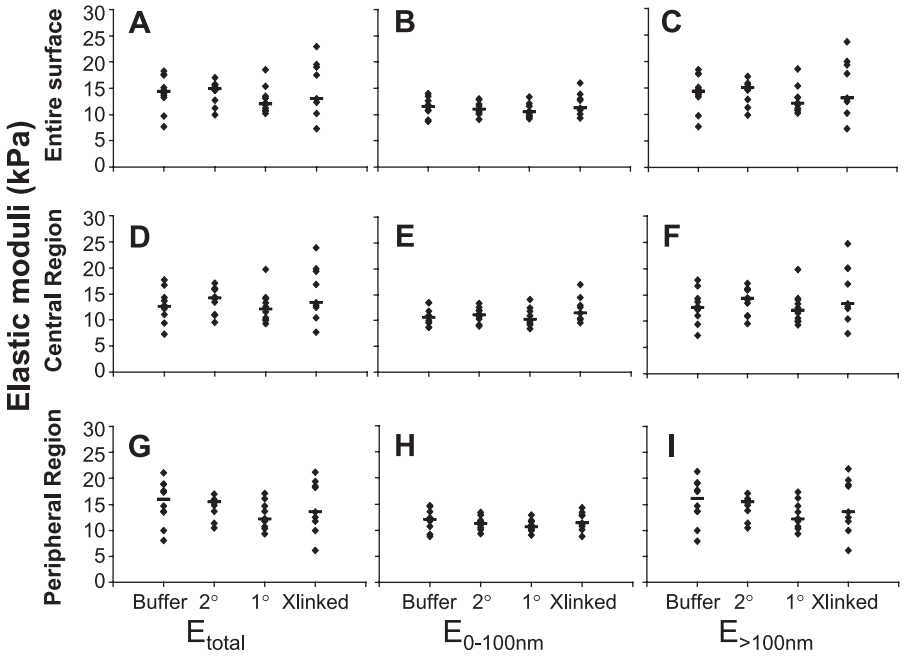

Figure 7. Elastic moduli of ECs before and after intercellular adhesion molecule (ICAM)–1 crosslinking. The median E_{total} (*A*), $E_{0–100\ nm}$ (*B*), and $E_{>100\ nm}$ (*C*) were determined over the entire surface of each EC for ICAM-1 crosslinked ECs (Xlinked), and for control groups treated with buffer only, secondary antibodies only, or primary antibodies only (Buffer, 2°, and 1°, respectively). Similarly, the median E_{total}, $E_{0–100\ nm}$, and $E_{>100\ nm}$ of ICAM-1 crosslinked ECs and control groups were determined in the central (*D–F*) and peripheral (*G–I*) regions for each EC. No significant difference was found between the ICAM-1 crosslinked ECs and the three control groups in any indentation depth or any region (n = 10, 10, 10, and 9 ECs from 3 monolayers for Buffer, 2°, 1°, and Xlinked groups, respectively).

by crosslinking ICAM-1 was not sufficient to induce significant changes in stiffness.

After neutrophil adhesion, the stiffness of ECs was initially decreased in the regions within 0–6.25 μm from the adherent neutrophils as soon as firm adhesion was detected. The changes induced by neutrophils were not present when averaged over the entire surface of ECs, indicating that these changes were localized to the regions, and not induced globally. Previously, Riethmuller and colleagues (14) measured the stiffness of leukocyte–endothelial interface after glutaraldehyde fixation, followed by removing adherent leukocytes by using the AFM tip. They did not detect a change in the stiffness at the leukocyte–EC interface, which could be due to the transient nature of the mechanical changes that cannot be detected after fixation.

It is possible that the changes in regions within 0–6.25 μm from the adherent neutrophils (rim 1) might be due to the extension of thin lamellipodia from neutrophils that are less than 1-μm thick. However, it is very unlikely that a lamellipodia would occupy the entire 6.25- × 6.25-μm pixel. Because the elastic modulus was determined at the center of the pixel, the lamellipodia (usually measuring 1–2 μm) would have needed to extend over 3 μm before they would be included in the measurement.

Intriguingly, neutrophil adhesion to an EC induced changes in the neighboring ECs within 1 minute that resulted in increased stiffness. This increase was observed in every adjacent EC from which we could obtain AFM measurements. This change was particularly significant in the central regions, although there was a strong trend in the periphery as well, so that this change was actually more diffuse than the changes in the EC to which the neutrophil was adherent. Furthermore, adherent neutrophils induced changes in the thickness of adjacent ECs. The mechanisms for both these changes in stiffness and in thickness are uncertain. The possibility that a neutrophil was touching the adjacent EC cannot be excluded. However, perhaps more likely are the possibilities that neutrophils are secreting a locally active signal to ECs, or that the ECs with adherent neutrophils are signaling to their neighbors, resulting in changes in stiffness and thickness. Because neutrophil adhesion and migration to the borders of ECs is usually in preparation for transmigration between ECs, these changes in adjacent cells may serve to facilitate this process. Furthermore, neutrophil adhesion can also be the predecessor for neutrophil-induced EC injury. In this light, it is interesting to note that Birukova and colleagues (15) measured the changes in elastic moduli in the periphery (Ep) and in the center (Ec) of human pulmonary artery ECs during stimulation with barrier-disruptive or barrier-enhancing agonists. They showed that barrier-disruptive agonists induced a decrease in the ratio of Ep:Ec, whereas barrier-enhancing agonists induced an increase in the ratio of Ep:Ec. The changes that we observed in adjacent ECs may be the earliest step in disruption of the endothelial barrier induced by adherent neutrophils.

The median E_{total} of TNF-α–treated ECs were 14 (±4) kPa in the present study, which is comparable to the elastic moduli of ECs reported in other AFM studies of ECs, ranging from 0.5 to 10 kPa (16–19). Reported values of elastic moduli of ECs show large variability, between 0.1 and 1 kPa when measured by micropipette aspiration (20–22), and less than 0.1 kPa when measured by magnetic bead twisting cytometry (1, 2, 23–25). The wide range of these values likely results from the different technologies and experimental conditions used for each type of measurement, including probe size, amount and type of applied force, and whether cell receptors are required for the measurement. The elastic moduli increased by an order of magnitude when measured by probes bound to the receptors linked to cytoskeleton compared with the stiffness measured by using non-cytoskeleton linked receptors, such as transferrin and acetyl low-density lipoprotein receptor (26, 27). Similarly, the degree of contact between the probe and the cell also affects the stiffness, as shown by a decrease in stiffness when the number of incompletely bound probes was increased (28). The amount and type of applied force also affects the resulting value of stiffness. Cells appear stiffer when higher stress is applied, or when a lateral shear force is applied in the horizontal direction instead of a twisting torque (23, 24). The mechanical response of the crosslinked actin network is dependent on the applied stress, so that the elasticity increases as strain becomes greater (29, 30). Thus, the high values of elastic moduli observed in the present study may be due to the high stress applied to the cells during the measurement of force-displacement curves with AFM, which is in the order of 5 kPa, as well as to the mechanical models used in calculating the elastic moduli, which tend to overestimate the elastic moduli due to the effect of rigid substrates (10, 31).

The elastic moduli depended on the indentation depths that were used to calculate E, and on the region. The median $E_{>100\ nm}$ of the TNF-α–treated ECs was significantly greater than $E_{0–100\ nm}$ in the peripheral and central regions. Moreover, the median $E_{0–100\ nm}$ was significantly greater in the peripheral regions than in the central regions. These data suggest that the mechanical properties of TNF-α–treated ECs appear different when probing 0- to 100-nm indentations than those greater than 100 nm. The differences between $E_{>100\ nm}$ and $E_{0–100\ nm}$ may be due to increased substrate effects at larger indentations, which were not considered in Hertz's model used in the present study. However, the differences between $E_{0–100\ nm}$ in the peripheral and central regions is not likely due to the significantly greater thickness of the central regions compare with the peripheral regions (1.86 ± 0.18 μm and 1.41 ± 0.16 μm, respectively; $P < 0.01$) for several reasons. First, the correlation between the elastic moduli of ECs and the thickness is very weak ($y = -4.5176x + 41889$, where y is the elastic moduli in Pa, and x is the thickness in nanometers; $R^2 = 0.0043$). Second, if the elastic moduli appeared stiffer due to increased substrate effect, then the difference would appear greater for $E_{>100\ nm}$ than for $E_{0–100\ nm}$, which was not the case. One possible explanation for the difference in $E_{0–100\ nm}$ of the peripheral and central regions is that the distribution of subcellular structures, such as organelles and cytoskeleton, which affect the mechanical properties, may differ in these regions.

The application of a stress to living cells can itself induce changes in mechanical properties. Other investigators have reported strain-induced hardening in cells, indicating that the application of force alone may induce stiffening of the cells (24, 32). However, changes in apparent moduli of ECs were not observed after repeated measurements of force-displacement relationships without adding neutrophils (data not shown) or after neutrophil adhesion, despite a large amount of applied force. These data indicate that the force applied during measurement alone did not induce changes in mechanical properties of ECs.

ICAM-1 crosslinking did not induce significant changes in the stiffness of pulmonary microvascular ECs, suggesting that the changes in EC stiffness induced by neutrophil adhesion may require more than ICAM-1 crosslinking. ICAM-1 crosslinking occurs globally in the entire surface of ECs, whereas ICAM-1 ligation during neutrophil adhesion occurs only at the site of neutrophil adhesion. Moreover, the changes in mechanical properties of ECs induced by neutrophils occurred within 5 minutes of adhesion, which might have been missed in the ICAM-1 crosslinking experiments, which took approximately 20 minutes for capturing each image. Furthermore, the ICAM-1 ligation is only one of many processes that occur during the adhesion and migration of neutrophils on ECs, and other molecular mechanisms that occur during the interaction between neutrophils and ECs may be responsible for the changes in elastic moduli

of ECs induced by neutrophil adhesion, when measured by AFM.

Our findings differ from the previous observations measured by magnetic bead twisting cytometry (1, 2), where both neutrophil adhesion and ICAM-1 crosslinking induced an increase in pulmonary microvascular EC stiffness. The difference in these results may be due to differences in contact area, the type and amount of applied forces, or other changes induced by ICAM-1 that might have affected the stiffness, such as an increase in the contact area or the number of β1-integrin bonds between the magnetic bead and ECs. In the magnetic bead twisting cytometry, the stress is applied through spherical probes of 4.5 μm in diameter that are bound to β1-integrin on ECs, and this stress consists of a torque of 21 dyne/cm^2 or 2.1 Pa. The stiffness measured by magnetic bead twisting cytometry is dependent on the contact area between the ferromagnetic bead and ECs. In AFM, a blunt-conical rigid probe of 100 nm in tip radius and 37.5° of half-open angle was used to apply a compressive pressure of approximately 5 kPa. Moreover, the contact area between the magnetic bead and EC is in the order of a few square microns, compared with a maximum of approximately 0.25 μm^2 during AFM nanoindentation.

In conclusion, our study demonstrates that neutrophil adhesion induces local changes in the stiffness of pulmonary microvascular ECs and more diffuse changes in the stiffness of adjacent ECs. This change was not mimicked by ICAM-1 crosslinking, suggesting that ICAM-1 crosslinking is not sufficient to induce these changes, or that focal ligation of ICAM-1 results in changes that are not observed after ligation of this molecule over an entire monolayer of ECs. The changes induced by neutrophil adhesion may require molecular mechanisms during interactions between neutrophils and ECs other than or in addition to ICAM-1 ligation.

Author Disclosure: I.K. has received sponsored grants ($50,000–$100,000) from the American Heart Association. None of the other authors has a financial relationship with a commercial entity that has an interest in the subject of this manuscript.

References

1. Wang Q, Chiang ET, Lim M, Lai J, Rogers R, Janmey PA, Shepro D, Doerschuk CM. Changes in the biomechanical properties of neutrophils and endothelial cells during adhesion. *Blood* 2001;97:660–668.
2. Wang Q, Doerschuk CM. Neutrophil-induced changes in the biomechanical properties of endothelial cells: roles of ICAM-1 and reactive oxygen species. *J Immunol* 2000;164:6487–6494.
3. Wang Q, Yerukhimovich M, Gaarde WA, Popoff IJ, Doerschuk CM. Mkk3 and -6–dependent activation of p38alpha MAP kinase is required for cytoskeletal changes in pulmonary microvascular endothelial cells induced by ICAM-1 ligation. *Am J Physiol Lung Cell Mol Physiol* 2005;288:L359–L369.
4. Marchant RE, Kang I, Sit PS, Zhou Y, Todd BA, Eppell SJ, Lee I. Molecular views and measurements of hemostatic processes using atomic force microscopy. *Curr Protein Pept Sci* 2002;3:249–274.
5. Radmacher M. Measuring the elastic properties of living cells by the atomic force microscope. *Methods Cell Biol* 2002;68:67–90.
6. Kataoka N, Iwaki K, Hashimoto K, Mochizuki S, Ogasawara Y, Sato M, Tsujioka K, Kajiya F. Measurements of endothelial cell-to-cell and cell-to-substrate gaps and micromechanical properties of endothelial cells during monocyte adhesion. *Proc Natl Acad Sci USA* 2002;99:15638–15643.
7. Cuerrier CM, Benoit M, Guillemette G, Gobeil F Jr, Grandbois M. Real-time monitoring of angiotensin II–induced contractile response and cytoskeleton remodeling in individual cells by atomic force microscopy. *Pflugers Arch* 2009;457:1361–1372.
8. Titushkin I, Cho M. Modulation of cellular mechanics during osteogenic differentiation of human mesenchymal stem cells. *Biophys J* 2007;93:3693–3702.
9. Collinsworth AM, Zhang S, Kraus WE, Truskey GA. Apparent elastic modulus and hysteresis of skeletal muscle cells throughout differentiation. *Am J Physiol Cell Physiol* 2002;283:C1219–C1227.
10. Mahaffy RE, Park S, Gerde E, Kas J, Shih CK. Quantitative analysis of the viscoelastic properties of thin regions of fibroblasts using atomic force microscopy. *Biophys J* 2004;86:1777–1793.
11. Briscoe BJ, Sebastian KS, Adams MJ. The effect of indenter geometry on the elastic response to indentation. *J Phys D Appl Phys* 1994;27:1156–1162.
12. Lagarias JC, Reeds JA, Wright MH, Wright PE. Convergence properties of the Nelder-Mead simplex method in low dimensions. *SIAM J Optim* 1998;9:112–147.
13. Brett J, Gerlach H, Nawroth P, Steinberg S, Godman G, Stern D. Tumor necrosis factor/cachectin increases permeability of endothelial cell monolayers by a mechanism involving regulatory G proteins. *J Exp Med* 1989;169:1977–1991.
14. Riethmuller C, Nasdala I, Vestweber D. Nano-surgery at the leukocyte–endothelial docking site. *Pflugers Arch* 2008;456:71–81.
15. Birukova AA, Arce FT, Moldobaeva N, Dudek SM, Garcia JG, Lal R, Birukov KG. Endothelial permeability is controlled by spatially defined cytoskeletal mechanics: atomic force microscopy force mapping of pulmonary endothelial monolayer. *Nanomedicine* 2009;5:30–41.
16. Sato M, Nagayama K, Kataoka N, Sasaki M, Hane K. Local mechanical properties measured by atomic force microscopy for cultured bovine endothelial cells exposed to shear stress. *J Biomech* 2000;33:127–135.
17. Rotsch C, Braet F, Wisse E, Radmacher M. AFM imaging and elasticity measurements on living rat liver macrophages. *Cell Biol Int* 1997;21:685–696.
18. Mathur AB, Collinsworth AM, Reichert WM, Kraus WE, Truskey GA. Endothelial, cardiac muscle and skeletal muscle exhibit different viscous and elastic properties as determined by atomic force microscopy. *J Biomech* 2001;34:1545–1553.
19. Miyazaki H, Hayashi K. Atomic force microscopic measurement of the mechanical properties of intact endothelial cells in fresh arteries. *Med Biol Eng Comput* 1999;37:530–536.
20. Byfield FJ, Aranda-Espinoza H, Romanenko VG, Rothblat GH, Levitan I. Cholesterol depletion increases membrane stiffness of aortic endothelial cells. *Biophys J* 2004;87:3336–3343.
21. Theret DP, Levesque MJ, Sato M, Nerem RM, Wheeler LT. The application of a homogeneous half-space model in the analysis of endothelial cell micropipette measurements. *J Biomech Eng* 1988;110:190–199.
22. Sato M, Ohshima N, Nerem RM. Viscoelastic properties of cultured porcine aortic endothelial cells exposed to shear stress. *J Biomech* 1996;29:461–467.
23. Bausch AR, Hellerer U, Essler M, Aepfelbacher M, Sackmann E. Rapid stiffening of integrin receptor-actin linkages in endothelial cells stimulated with thrombin: a magnetic bead microrheology study. *Biophys J* 2001;80:2649–2657.
24. Pourati J, Maniotis A, Spiegel D, Schaffer JL, Butler JP, Fredberg JJ, Ingber DE, Stamenovic D, Wang N. Is cytoskeletal tension a major determinant of cell deformability in adherent endothelial cells? *Am J Physiol* 1998;274:C1283–C1289.
25. Wang Q, Doerschuk CM. The p38 mitogen-activated protein kinase mediates cytoskeletal remodeling in pulmonary microvascular endothelial cells upon intracellular adhesion molecule–1 ligation. *J Immunol* 2001;166:6877–6884.
26. Wang N, Ingber DE. Probing transmembrane mechanical coupling and cytomechanics using magnetic twisting cytometry. *Biochem Cell Biol* 1995;73:327–335.
27. Huang H, Kamm RD, So PT, Lee RT. Receptor-based differences in human aortic smooth muscle cell membrane stiffness. *Hypertension* 2001;38:1158–1161.
28. Fabry B, Maksym GN, Hubmayr RD, Butler JP, Fredberg JJ. Implications of heterogeneous bead behavior on cell mechanical properties measured with magnetic twisting cytometry. *J Magn Magn Mater* 1999;194:120–125.
29. Gardel ML, Shin JH, MacKintosh FC, Mahadevan L, Matsudaira P, Weitz DA. Elastic behavior of cross-linked and bundled actin networks. *Science* 2004;304:1301–1305.
30. Storm C, Pastore JJ, MacKintosh FC, Lubensky TC, Janmey PA. Nonlinear elasticity in biological gels. *Nature* 2005;435:191–194.
31. Dimitriadis EK, Horkay F, Maresca J, Kachar B, Chadwick RS. Determination of elastic moduli of thin layers of soft material using the atomic force microscope. *Biophys J* 2002;82:2798–2810.
32. Wang N, Butler JP, Ingber DE. Mechanotransduction across the cell surface and through the cytoskeleton. *Science* 1993;260:1124–1127.